The transmitter pointing determination in the Geoscience Laser Altimeter System

J. Marcos Sirota,[1] Sungkoo Bae,[2] Pamela Millar,[3] David Mostofi,[1] Charles Webb,[2] Bob Schutz,[2] and Scott Luthcke[3]

[1] The determination of accurate elevation data using laser altimetry relies on accurate knowledge of the instrument pointing angle. The Geoscience Laser Altimeter System (GLAS) on the Ice, Cloud and land Elevation Satellite (ICESat) uses a novel system for determination of the laser pointing vector. In this paper we describe this system, as well as the method used to process its data, which are required to meet ICESat's science objectives. We discuss the necessary modifications to processing techniques, implemented to optimize accuracy for the various operating conditions. Results to date are compared to calibration/validation data to assess their accuracy. We show that the stated requirements have been met for near nominal operating conditions. **Citation:** Sirota, J. M., S. Bae, P. Millar, D. Mostofi, C. Webb, B. Schutz, and S. Luthcke (2005), The transmitter pointing determination in the Geoscience Laser Altimeter System, *Geophys. Res. Lett.*, *32*, L22S11, doi:10.1029/2005GL024005.

1. Introduction

[2] Achieving ICESat's science objective of measuring 2.0 cm/year elevation change averaged over 100 km × 100 km areas [*Zwally et al.*, 2002] requires accurate determination of the surface elevation of each laser footprint, as well as its precise geolocation. The location of the GLAS footprint and its associated elevation are obtained by combining the geocentric position vector of the GLAS instrument with a range vector formed by the scalar distance to the surface, inferred from the round-trip travel time of the laser pulse, and the laser-pointing direction, ascertained through precision attitude determination (PAD). With a 600 km spacecraft altitude, a one arcsecond uncertainty in the laser pointing direction produces a 5 cm single shot range error over a surface slope of 1°. To achieve the mission science requirements, it is necessary to determine the laser beam pointing direction to better than 1.5 arcsecond (1σ) [*Zwally et al.*, 2002].

[3] PAD is accomplished through Extended Kalman Filter (EKF) processing of instrumental data gathered with the on-board Stellar Reference System (SRS). Here we present the SRS used for the determination of the outgoing laser pointing vector in inertial space, a description of the current PAD processing method, the limitations imposed on its accuracy by the current off nominal operating conditions, and some calibration/validation results. Our analysis is limited to the Laser 2a (L2a) operations period, which is the most completely processed operational period to date and during which the GLAS instrument operated at near nominal conditions. We compare here results obtained with data Release 12 and data Release 19. We briefly discuss the Laser 2b (L2b), Laser 2c (L2c) and Laser 3a (L3a) operations periods.

2. Stellar Reference System

[4] A conceptual diagram of the SRS is shown in Figure 1. The concept relies on a classical high accuracy Attitude Determination System (ADS) coupled to a novel laser reference camera using an active optical fiducial. The ADS measures the pointing of the GLAS instrument platform with respect to the star field while the laser reference sensor (LRS) samples the laser beam at 10 Hz and measures its alignment with respect to the components of the ADS. The Laser Profiling Array (LPA) measures the far field spatial pattern of the laser beam energy at 40 Hz, the laser firing frequency.

[5] The ADS devices in the SRS are an HD-1003 instrument star tracker (IST), and the inertial reference unit (IRU), which consists of four Hemispherical Resonator Gyros (HRG). The IST is capable of observing up to 6 stars simultaneously with an 8° field of view (FOV). The star measurements from the IST and the angular rates from the HRG are used to determine the ADS attitude at a 10 Hz rate.

[6] A sample of the GLAS laser beam is sent into the laser reference sensor FOV with two lateral transfer retro-reflectors. The LRS consists of a narrow FOV camera (8.5 × 8.5 mrad) operating at 10 Hz frame rate. The camera includes a Newtonian telescope and a modified star tracker that images and computes the centroid of the GLAS laser beam, of stars, and of the alignment fiducial referred to as the collimated reference source (CRS) [*Sirota et al.*, 2001]. The CRS is rigidly mounted to the star-tracker housing to monitor the star-tracker alignment with respect to the LRS. The CRS uses an optical fiber to focus a split fraction of 532 nm laser pulse energy that is produced by frequency-doubling the 1064 nm output of the GLAS lasers used for profiling of atmospheric clouds and aerosols [*Abshire et al.*, 2005]. The LRS also images stars every few minutes, which yields a boresight check between the LRS and the star-tracker. The LPA is an 80 × 80 pixel array imager with the same FOV per pixel as the LRS and operates at 40 Hz, to image every transmitted laser pulse.
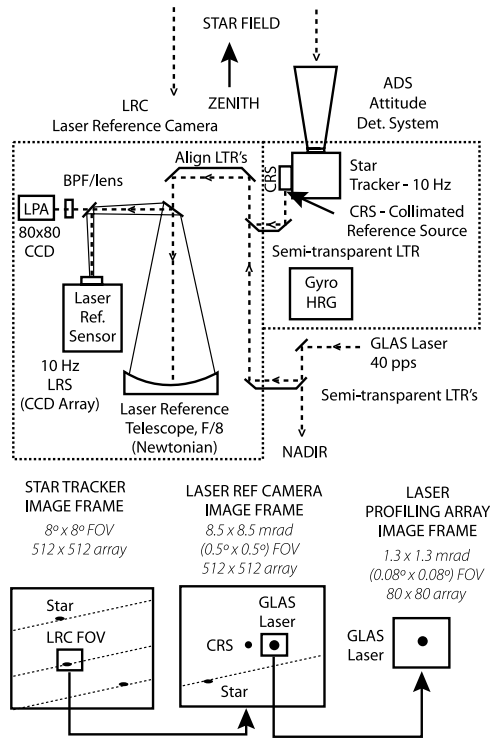
3. SRS Data Processing - PAD

[7] The overlap of the SRS detectors' fields of view is shown in Figure 1. In order to relate the various pointing

[1]Sigma Space Corp, Lanham, Maryland, USA.
[2]University of Texas Center for Space Research, Austin, Texas, USA.
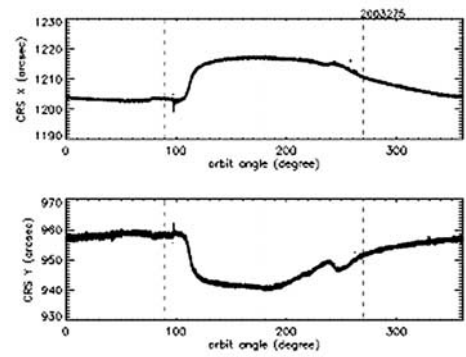[3]NASA Goddard Space Flight Center, Greenbelt, Maryland, USA.

Figure 1. GLAS Stellar Reference System conceptual approach.

Figure 2. Orbital variation of CRS centroid in LRS FOV for both axes, representing relative motion between IST and LRS for an entire orbit. Absolute scale represents position of the CRS (or IST boresight) within LRS field of view. The approximately 20 arcsec variation per axis per orbit can be seen. If unaccounted for, this variation would severely limit mission accuracy.

vectors to the ADS attitude solution, simple translation/rotation operations are applied [*Bae et al.*, 2002]. The attitude of the IST is defined as a matrix $A(t)$ that transforms star observations from the celestial reference frame (CRF) to the IST coordinate frame, and is determined from the EKF processing of the IST and HRG data.

[8] By design, the relative alignment between LRS and IST could be determined either by simultaneous observations of stars in both fields of view, or by the motion of the centroid of the CRS in the LRS image frame. This dual method was designed into the system as a measurement/verification approach to minimize errors in the measurement of the unavoidable thermal motion between the two sensors. The original software developed for PAD relied on occasional simultaneous star observations in the FOV of the IST and LRS to align the two frames by simple translation/rotation, while using the CRS as a cross check of proper co-alignment information between both cameras for periods where stars were not simultaneously present in both fields. Unfortunately, a stray light issue with the sunshade of the LRS precluded observation of stars, with this sensor, on the day side of the orbit. Therefore, the PAD software was modified to continuously determine the laser-pointing vector using the CRS information, leaving the LRS star information as a cross check [*Bae et al.*, 2004].

[9] It was anticipated during design, as well as proven during pre-launch testing, that the IST-LRS co-alignment was strongly dependent on temperature. It was verified during the early stages of the mission that the CRS centroids produced a characteristic orbital signature, corresponding to thermally induced motion of the IST, in the FOV of the LRS, as shown in Figure 2. These data indicate variations in coalignment between the two cameras of the order of 20 arcsecond per orbital period, which underscores the

importance of the fiducial CRS information, since otherwise this motion would be unaccounted for, and directly impacts the accuracy of the PAD and subsequently the altimetry.

[10] The plate scale of the LRS and LPA (3.4 arcsec per pixel) permit acquisition of laser pointing information with sub-arcsecond resolution. Figure 3 shows a typical signature of the laser centroids on the LRS for several orbits. The orbital variation is about 2 arcsec peak to peak per axis and presents two peaks per orbit that coincide with the passes through terminator for the spacecraft. These complex motions of the laser vector and of the IST with respect to the LRS illustrate the importance of the pointing monitoring devices.
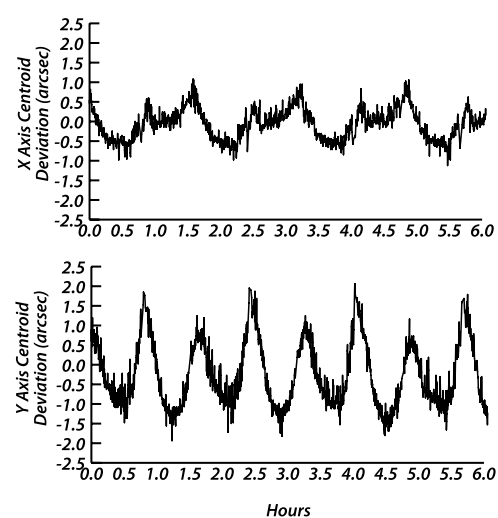
Figure 3. Laser Centroid as function of time in LRS. The orbital (approx. 1.5 hour cycle) laser motion of a few arcsec per axis is evident, and also secondary peaks which correspond to the pass through terminator are clearly captured.

[11] The spatial distribution of laser energy is imaged using the LPA and the LRS, as both cameras employ high spatial resolution. Images for Lasers 1, 2 and 3 are shown in this issue [*Abshire et al.*, 2005]. The lasers have produced elliptical footprints with a central maximum and radial decrease in energy for the majority of GLAS operations. This simple geometry permits the use of the centroid as a very good representation of footprint geolocation.

[12] In the current PAD processing the LPA laser image is projected onto the LRS FOV by co-aligning the centroid of the LPA image and the on-board reported centroid of the laser image on the LRS. Then the CRS centroid information is used to align the LRS frame within the IST FOV. At this point, the laser is represented at 40 Hz with respect to the IST (or ADS) frame. Finally, using $A^{-1}(t)$, the pointing of the laser beam in the celestial reference frame (CRF) is obtained. It is important to note that despite the unavoidable relative motion between sensors in the optical bench, the optical fiducial design yields absolute pointing determination. The final pointing vector is determined by adding bias values, derived from calibration techniques, to the laser-in-CRF vector. The calibration bias angles have been obtained from averaged ocean sweep calibration maneuvers [*Luthcke et al.*, 2000]. Note that for the data releases used here for performance evaluation, Releases 12 and 19, a single fixed bias per orbit was applied.

4. Instrument Issues and Their Resolution

[13] The GLAS instrument's limited laser lifetime, due to both potential sudden permanent cease fire and energy decay more rapid than anticipated, and the consequent low temperature operation [*Abshire et al.*, 2005] has imposed a severe penalty on 532 nm energy output for all periods after L2a. Unfortunately, the light energy source for the CRS is a split fraction of the 532 nm beam focused into an optical fiber. Therefore the intensity of the CRS for L2b and L2c operations periods was low, and for L3a and L3b operations periods was virtually undetectable. For L2b, a smooth fitting to the noisy, intermittent data has been applied (Release 16). For L2c, L3a and L3b, it was determined empirically that 15-second averages of the images reported by the LRS for the CRS area yielded meaningful centroid information, at least for the eclipse side of the orbit. This baseline, plus a model based on L2a operation, will be applied to data for these operation periods. In spite of this issue innovative approaches to data processing are yielding solutions that approach the accuracy of the L2a period.

5. Calibration/Validation Techniques and Results

[14] At the ICESat Science Investigator-led Processing System (I-SIPS), the PAD data are combined with the precision orbit determination (POD) and laser-ranging data to produce estimates for each footprint location on the surface of the Earth, along with the topographic elevation at that point, through a process called geolocation [*Schutz*, 2002]. The geolocation results are reported in the location data given on the ICESat Level 2 data products (GLA06, GLA12 etc.).

[15] We assess the accuracy of our pointing solutions using ground validation data. For attitude systems in gen-
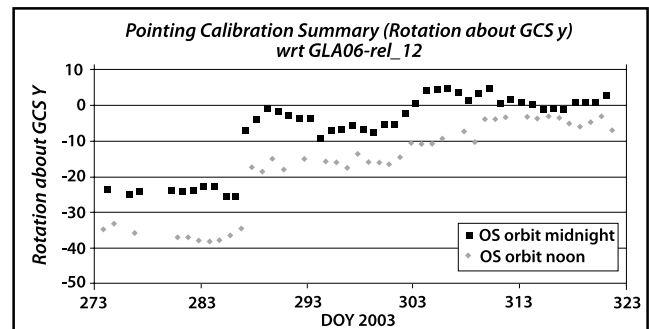
Figure 4. Pointing bias calibration results from ocean scans obtained without LRS data for complete L2a period when LRS data was not part of solution (Release 12). (GCS is GLAS Coordinate System).

eral, where an actual external "truth" cannot be applied, the error in the filtered solution is usually considered the accuracy of the attitude determination system. In our case, we can compare the pointing determination solution to either few point measurements for laser footprint landing on the ground, or multiple footprint comparisons using well-known angular biases and ground slopes. Absolute evaluation of the transmitted pulse pointing determination accuracy requires physically registering laser footprint landings on the ground, albeit footprint location determination yields geolocation, and this is the result of POD, timing, and PAD. However, the errors of POD and timing are fairly small in comparison to potential error in geolocation introduced by pointing determination errors. The direct techniques applied to date are ground-based active detection [*Magruder et al.*, 2005] which relies on a large set of photodiodes spread on the ground, and look-up ground photography [*Sirota et al.*, 2004], consisting of multiple cameras photographing the green beam from the ground looking up and analyzing relative intensities to determine a centroid for the spot. Both have demonstrated that the SRS solution for L2a is accurate to within 5 arcsec and 2 arcsec respectively. However, due to mission operational limitations very few direct measurements of pointing were obtained in both of those works, thus their statistical significance is limited.

[16] Pointing calibration techniques based on GLAS range measurements are the most commonly applied since they rely only on on-board data and independent knowledge of surface elevations, and do not require specific ground installations. Of the ranging based techniques, Integrated Residual Analysis using ocean scans (OS) and cross-overs [*Luthcke et al.*, 2000] is the most widely applied. We concentrate here on results provided by that technique. However, we note that pointing errors introduced in the receiver path, such as those due to receiver boresight misalignment, are included in the total pointing error established by this method because they are indistinguishable from transmitter PAD bias errors [*Luthcke et al.*, 2005].

[17] For ICESat, calibration OS maneuvers with a 5 degree off-nadir amplitude are conducted twice per day over the Pacific Ocean centered around the Equator, during ascending and descending passes. Range residuals with respect to the independently established elevation of the

ocean surface are analyzed to separate pointing biases from range, POD and timing biases. Results for the L2a operations period from OS calibration are shown in Figures 4 and 5, as rotational biases about the GLAS Coordinate System (GCS) Y-axis. Data for sun-illuminated and eclipse sides of the orbit are shown against day of the year. The X-axis data yields similar results. The Release-12 results, shown in Figure 5, are those obtained by using only the ADS solution without any LRS information. The laser direction is therefore calculated using a fixed bias between the axes of the tracker and the laser. Data was released in this form before SRS processing was fully implemented. A much better agreement between calibration data for day/night sides of the orbit is found, as shown in Figure 5 with Release 19, when the complete SRS data was applied. This solution takes into account the relative motion of the tracker with respect to the Laser Reference Sensor, and then also the motion of the Laser in the LRS field of view. A standard deviation of 1.3 arcsec per axis was found in the Release 19 data, which is compliant with the original requirement for the SRS system.

[18] For the pointing error results of this method, based on range measurements, to be only due to the attitude/SRS system requires that other sources of error do not introduce range residuals during the ocean scans. However, it was found for this instrument that misalignment between the laser beam and the altimeter receiver boresight, which causes FOV shadowing that has significant influence on the range residual pointing bias, is highly dependent on temperature. Therefore an orbital variation in pointing bias due to FOV shadowing is expected. Thus the 1.3 arcsec found so far constitutes an upper limit to the SRS error. The SRS contribution to the pointing error is in fact likely to be smaller. An ongoing effort to calibrate the receiver boresight error as a function of temperature, based on 532 nm channel boresight scans and data presented here [*Abshire et al.*, 2005], has shown that the residual error and trend still present in Release 19 is consistent with the magnitude of the receiver/transmitter misalignment for each axes.

6. Conclusions

[19] The determination of transmitter pointing by means of celestial reference with the SRS apparatus has proven effective and compliant with original requirements when the instrument operated at nominal conditions (L2a). The redundancy and cross checks of the system have provided reliability even when some of the components performed sub-optimally. Even when systems external to the SRS have failed (i.e., the laser light source used by the CRS), the somewhat repetitive orbital behavior of the system provides a basis for appropriate modeling and for approximate solutions.

[20] It has been shown [*Luthcke et al.*, 2005] that during the period of nominal operating conditions (L2a) the accuracy demonstrated by the transmitter pointing solutions is sufficient to detect ice sheet elevation change once receiver misalignment error is removed. In addition, the high spatial resolution images of the laser beam have proven useful for modeling received echo waveforms [e.g., *Harding and Carabajal*, 2005], as well as engineering analysis and diagnosis of laser issues [*Abshire et al.*, 2005].
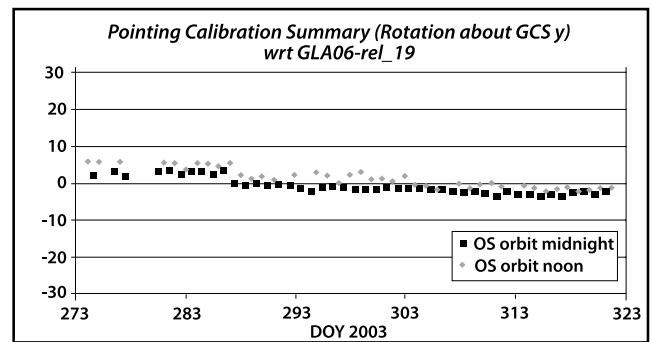
Figure 5. Pointing bias calibration results from ocean scans obtained with LRS data for complete L2a period using Release 19 data.

[21] The current pointing determination system complies with requirements, and the various GLAS instrument issues provide invaluable information for the identification of additional features or necessary modifications for pointing determination systems to be applied in future missions.

References

Abshire, J. B., X. Sun, H. Riris, M. Sirota, J. McGarry, S. Palm, D. Yi, and P. Liiva (2005), Geoscience Laser Altimeter System (GLAS) on the ICESat Mission: On-orbit measurement performance, *Geophys. Res. Lett.*, *21*, L21S02, doi:10.1029/2005GL024028.

Bae, S., B. Schutz, and J. M. Sirota (2002), ICESat/GLAS laser pointing determination, in *Spaceflight Mechanics*, *Adv. Astronaut. Sci.*, vol. 112, edited by K. T. Alfriend, pp. 359–370, Univelt, San Diego, (Calif.

Bae, S., C. Webb, and B. Schutz (2004), GLAS PAD calibration using laser reference sensor data, paper presented at *AIAA/AAS Astrodynamics Specialist Conference and Exhibit*, Am. Inst. of Aeronatu. and Astrnonaut., Providence, R. I.

Harding, D. J., and C. C. Carabajal (2005), ICESat waveform measurements of within-footprint topographic relief and vegetation vertical structure, *Geophys. Res. Lett.*, *32*, L21S10, doi:10.1029/2005GL023471.

Luthcke, S., D. Rowlands, J. McCarthy, D. Pavlis, and E. Stoneking (2000), Spaceborne laser-altimeter-pointing bias calibration from range residual analysis, *J. Spacecr. Rockets*, *27*, 374–384.

Luthcke, S. B., D. D. Rowlands, T. A. Williams, and M. Sirota (2005), Reduction of ICESat systematic geolocation errors and the impact on ice sheet elevation change detection, *Geophys. Res. Lett.*, *32*, L21S05, doi:10.1029/2005GL023689.

Magruder, L., E. Silverberg, C. Webb, and B. Schutz (2005), In situ timing and pointing verification of the ICESat altimeter using a ground-based system, *Geophys. Res. Lett.*, *21*, L21S04, doi:10.1029/2005GL023504.

Schutz, B. (2002), Laser Footprint Location (Geolocation) and Surface Profiles, GLAS Algorithm Theoretical Basis Document, version 3.0, NASA Goddard Space Flight Cent., Greenbelt, Md. (Available at: http://www.csr.utexas.edu/glas/pdf/atbd_geoloc_10_02.pdf.)

Sirota, J. M., P. Millar, E. Ketchum, B. Schutz, and S. Bae (2001), System to attain accurate pointing knowledge of the Geoscience Laser Altimeter, in *Guidance and Control 2001*, *Adv. Astronaut. Sci.*, vol. 107, edited by R. D. Culp and C. N. Schira, pp. 39–48, Univelt, San Diego, Calif.

Sirota, J. M., P. Millar, C. T. Field, D. K. Mostofi, E. Ketchum, C. Carabajal, and S. Luthcke (2004), Laser pointing determination system for the Geoscience Laser Altimeter on ICESat: Initial in-flight performance assessment, in *Guidance and Control 2004*, *Adv. Astronaut. Sci.*, vol. 118, pp. 607–622, Univelt, San Diego, Calif.

Zwally, J., et al. (2002), ICESat's laser measurements of polar ice, atmosphere, ocean and land, *J. Geodyn.*, *34*, 405–445.

————————————
S. Bae, B. Schutz, and C. Webb, University of Texas Center for Space Research, Austin, TX 78759–5321, USA.

S. Luthcke and P. Millar, NASA Goddard Space Flight Center, Space Geodesy Laboratory, Code 697, Greenbelt, MD 20771, USA.

D. Mostofi and J. M. Sirota, Sigma Space Corp, 4801 Forbes Blvd., Lanham, MD 20706, USA. (marcos.sirota@sigmaspace.com)